Journal of Power Sources 195 (2010) 3333–3337

Contents lists available at ScienceDirect

Journal of Power Sources

journal homepage: www.elsevier.com/locate/jpowsour

Short communication

Free standing aluminum nanostructures as anodes for Li-ion rechargeable batteries

Ming Au[a,*], Scott McWhorter[a], Henry Ajo[a], Thad Adams[a], Yiping Zhao[b], John Gibbs[b]

[a] Savannah River National Laboratory, Aiken, SC, USA
[b] University of Georgia, Athens, GA, USA

ARTICLE INFO

Article history:
Received 19 October 2009
Received in revised form
19 November 2009
Accepted 25 November 2009
Available online 2 December 2009

Keywords:
Battery
Lithium
Nanostructure
Aluminum
Anode

ABSTRACT

The free standing aluminum nanorods were grown on electrode and evaluated electrochemically as the anodes in the half-cell of Li-ion battery. The average diameter and length of the nanorods are 80 nm and 200 nm, respectively. The aligned nanorods demonstrated high capacity of 1243 mAh g^{-1} at rate of 0.5 C. A gradual decrease of the initial capacity was observed. The characterization of the anodes shows that the changes of the crystalline structure and morphology during cycling may be responsible for the capacity decay. The appropriate selection of the substrate can overcome the problems and lead the sustainable high capacity.

1. Introduction

The capacity of carbon intercalation anodes used in Li-ion rechargeable batteries currently is limited to 372 mAh g^{-1} [1]. Ever growing demand on lighter, cheaper and safer Li-ion batteries with high energy density that can power electric vehicles and portable electronics stimulates researchers to discover new anode materials. A number of metals and metal oxides has been investigated for next generation of high capacity anodes [2–10]. However, the large volume expansion (300–400%) during metal-Li alloying or oxide-Li conversion causes pulverization of anode materials and results in rapid decrease of high capacity. Furthermore, these powdery metals and metal oxides must be mixed with conductive additives, binders and solvent before being pasted on current collectors. This conventional fabrication process is not only complicated and costly, but also limits the electron conductivity due to lack of direct contact of active materials and current collectors. Growing aligned nanostructures (i.e., nanorods) of active materials on the electrodes represents one of the solutions for above problem. The interstitial space in aligned nanorods (NRs) may accommodate the volume expansion of the NRs and provide more access sites for Li-ion shuttling that reduces the stress resulting in longer cycling life. Secondly, direct contact of the NRs and electrode significantly improves electronic conductivity, which will allow higher power density. Finally, the direct growing of active materials on electrodes eliminates multi-stepped mixing-pasting-pressing—baking process and reduces fabrication cost and mass of materials considerably. In this paper, we report the initial results of our investigation and discuss several interesting issues associated with increasing the cycleability of NR electrodes.

2. Experimental

A thin film of aligned aluminum NRs (Al NRs) was grown on the substrate using glancing angle deposition (GALD). GLAD is a physical vapor deposition technique that takes advantage of the "shadowing effect." If the angle between the incident vapor plume and the substrate surface is large (~86°), then the random initial nucleation points formed upon the surface of the substrate act as seeds for nanorod growth. As additional vapor accumulates on the substrate, its growth is restricted to those nucleation points due to the shadow cast by those points leading to an array of nanorods (Fig. 1). The details were reported in the previous publication [11]. A glass slide was coated with a homogenous Ti thin film as the substrate in a sputtering chamber. The morphology and structure of Al NRs were characterized by Hatichi C430 Scanning Electron Microscope (SEM) and Panalytical X'Pert Pro X-ray diffractometer (XRD), respectively. A baker cell of Li-ion battery was constructed in VAC

* Corresponding author at: Savannah River National Laboratory, Materials Science and Technology, 999-2w, Aiken, SC 29808, USA. Tel.: +1 803 507 8547; fax: +1 803 652 8137.
E-mail address: ming.au@srnl.doe.gov (M. Au).

0378-7753/$ – see front matter © 2009 Elsevier B.V. All rights reserved.
doi:10.1016/j.jpowsour.2009.11.102

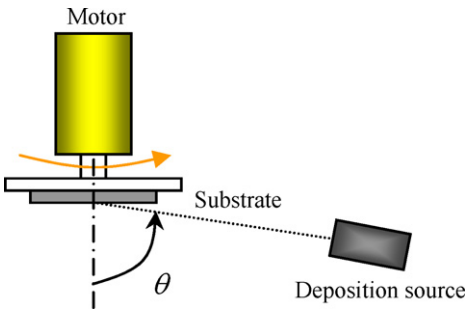

Fig. 1. Schematic of the glancing angle deposition.

glove box filled with argon. The Al NR anode coated slide and a Li foil (Aldrich) were inserted in the cell as the anode and cathode, respectively. The 1 M $LiPF_6$ in PC/DMC (propylene carbonate and dimethyl carbonate) was purchased from Ferro and used as the electrolyte. Princeton Applied Physics' VersaSTAT-3 was used for measurement of electrochemical properties of the new anodes. The galvanic charge–discharge was carried out at 700 mA g^{-1} from 0.01 V to 3.00 V. Cyclic voltammetry (CV) was measured at 0.1 mV s^{-1} from 0.01 V to 3.00 V. After 20 and 100 cycles, the anodes were taken out of the cell for SEM, XRD and XPS characterization. The surface chemistry of anode was investigated by Karator AXIS HSi X-ray photoelectron spectroscope (XPS).

3. Results and discussion

3.1. Materials characterization

SEM images show that the black thin film coated on Ti substrate is the aligned Al NRs. The average diameter and length of the NRs were 100 nm and 0.5 μm, respectively (Fig. 2). The electron dispersion spectroscopy (EDS) analysis confirms the NRs are pure Al (Figs. 3 and 4). X-ray diffraction (XRD) spectrum indicated that the aligned Al NRs have high textured orientation represented by a broad baseline (Fig. 5).

3.2. Electrochemical performance of the Al NRs anodes

A cyclic voltammogram of Li/Al NR cell is shown in Fig. 6. Two sets of similar current peaks (A_1–A_5 and B_1–B_5) appear in the first and second CV. Following an increase of the potential, the peaks of A_1 at 0.491 V may correspond to lithium reduction and formation of Li–Al solid solution. After Li^+ concentration increases and exceeds the limit of solubility (~0.5%), the low lithium alloy of LiAl [12] may form resulting in appearance of the peak A_2 at 0.841 V. Further charging will move more Li-ions into the Al that transforms LiAl to high lithium alloy as Li_9Al_4 [12]. The peak A_3 at 0.937 V may correspond to that. The proposed anode reactions could be written as

$$Li^+ + Al + e^- \rightarrow LiAl \quad (1)$$

$$5Li^+ + 5e^- + 4LiAl \rightarrow Li_9Al_4 \quad (2)$$

In the reverse process, the peak A_4 and A_5 may represent Li^+ oxidation when the potential was decreased gradually. The second CV repeats similar peaks B_1–B_5 that is evidence of the reversible Li^+ redox reactions. According to the reaction (2), the Al anode has 1411 mAh g^{-1} of theoretical capacity. In our case, the Al NR anode demonstrated 1243 mAh g^{-1} of capacity in the first discharge (Fig. 7) that is close to its theoretical prediction. It exhibits the potential of Al NRs as the high capacity anodes with low cost. However, the charging capacity decreased to 440 mAh g^{-1} in the second cycle. After 10 charging–discharging cycles, the reversible capacity decreased to 100 mAh g^{-1} (Fig. 8).

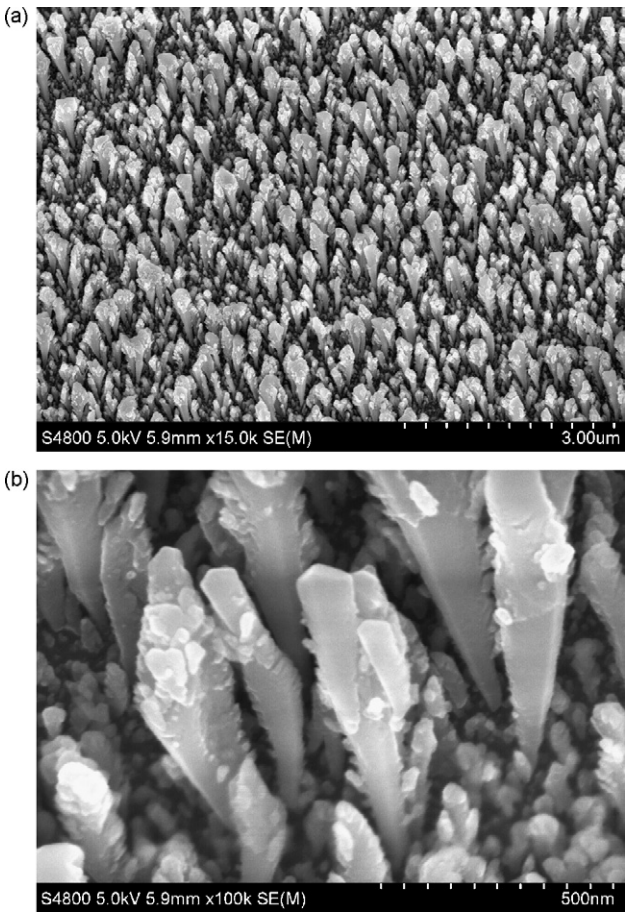

Fig. 2. (a) SEM image of the aligned Al NRs (15,000×) and (b) SEM image of the aligned Al NRs (100,000×).

3.3. Mechanism of capacity decay of Al NR anode

To understand the causes of the capacity decay, the SEM, XRD and XPS investigations were conducted. It was found that the Al NRs maintain their original aligned character, but the image was blurred due to the static charge accumulated after first discharge–charge cycle (Fig. 9) that implies poor electronic conductivity caused possibly by either Al oxidation or loss of contact of the Al NRs with the Ti substrate. After 20 cycles, most Al NRs merged into flakes (Fig. 10).

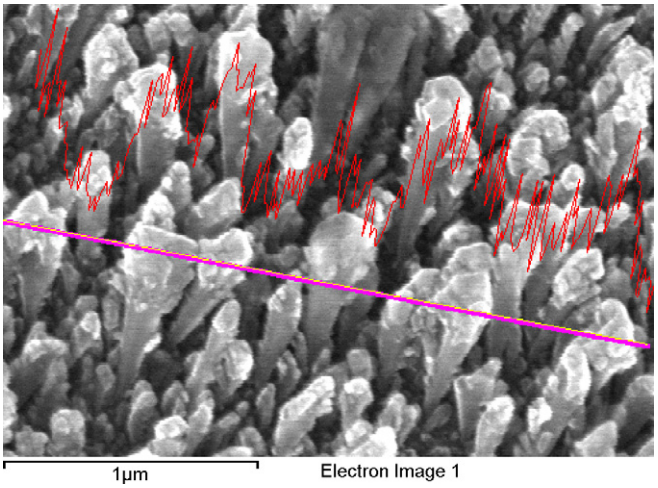

Fig. 3. EDS Al-line scan of the aligned Al NRs (50,000×).

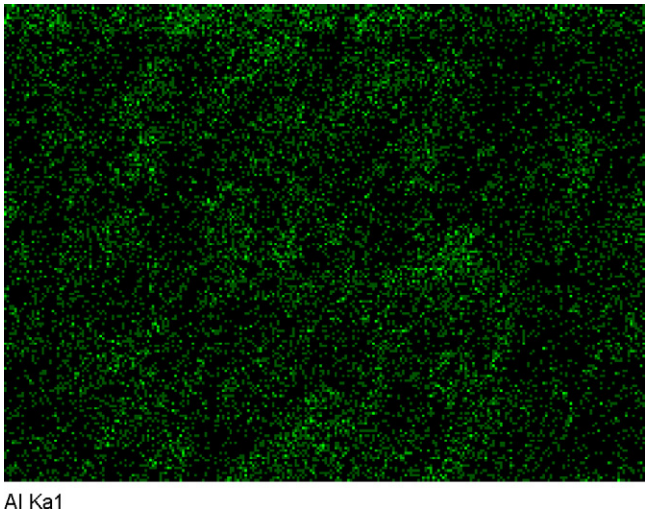

Fig. 4. EDS Al-map of the aligned Al NRs (50,000×).

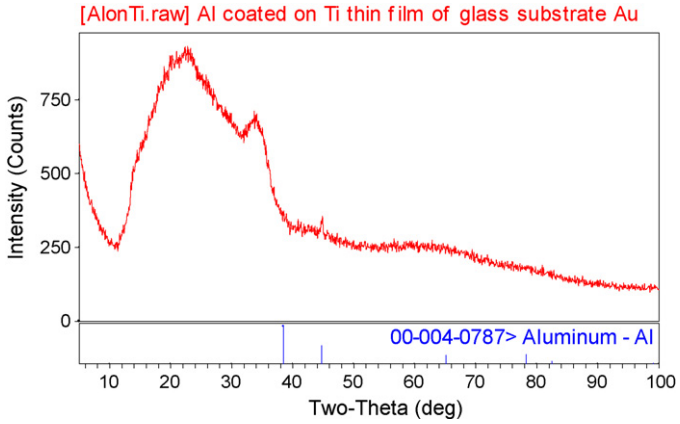

Fig. 5. X-ray diffraction (XRD) spectrum indicated that the aligned Al NRs have high textured orientation represented by a broad baseline.

After 100 cycles the original high capacity had almost diminished (Fig. 11) and the SEM image indicates that the Al NRs had collapsed into net like domains (Fig. 12). The cross sectional SEM shows that the Al layer was separated from Ti substrate that lost direct electrical contact (Fig. 13). XRD shows disappearance of the texture of aligned NRs and appearance of typical crystalline Al metal (Fig. 14).

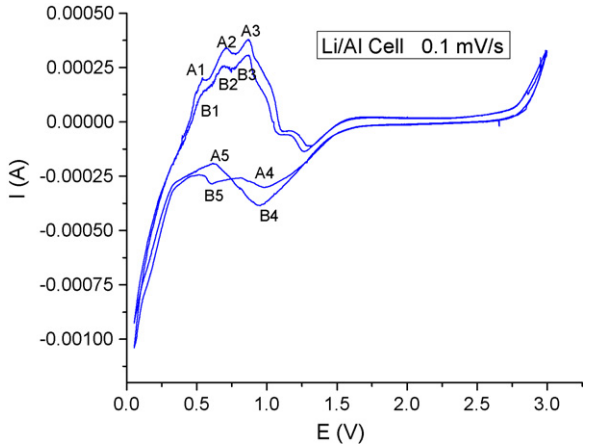

Fig. 6. A cyclic voltammogram of Li/Al NRs cell.

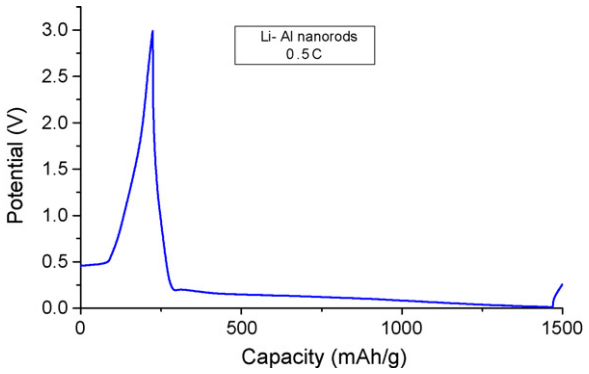

Fig. 7. The first discharge of Li/Al NRs cell.

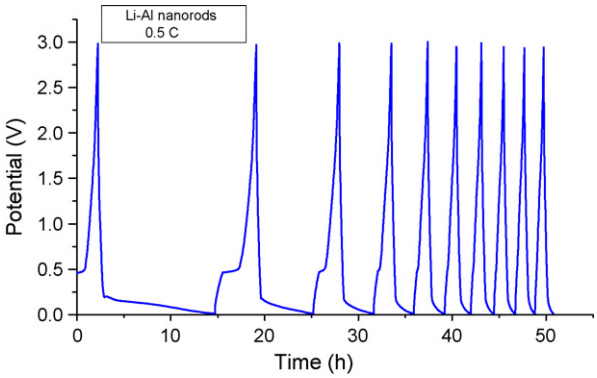

Fig. 8. The 10 charge–discharge cycles of Li/Al NRs cell.

It is well known that the nanostructure is metastable configuration thermodynamically. The nanostructure tends to agglomerate for reducing of its surface energy when the conditions are favorable. The unfavorable morphology and structure change results in poor electrical contact of Al and electrode and reduction of surface area.

XPS analysis shows that the surface of Al anode was oxidized. The Al peak shifted from 74.442 eV to 74.4 eV (Fig. 15). The oxidation could be caused by short exposure to air during sample transfer or by impurity of electrolyte. The surface oxidation may contribute little to large capacity decay.

To increase adhesion of Al with substrate and prevent Al NR layer from peeling off, the Ti substrate was replaced by other material. The galvanic cycling of Al NRs on new substrate shows that

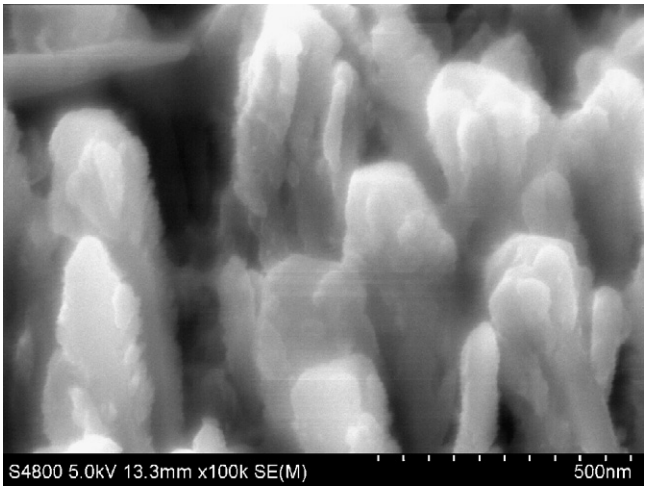

Fig. 9. SEM image of the Al NRs after first cycle (100,000×).

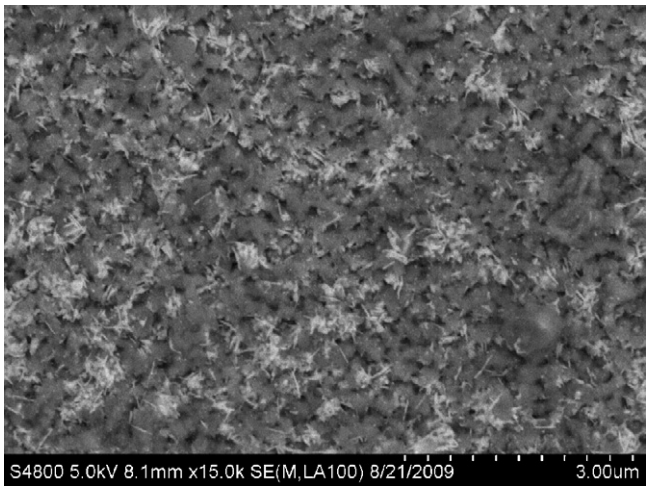

Fig. 10. SEM image of the Al NRs after 20 cycle (15,000×).

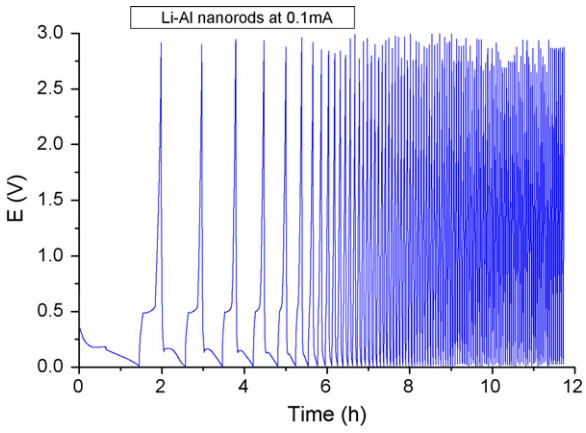

Fig. 11. The capacity decay of Al NRs in 100 cycles.

the first discharge and charge capacities were 1200 mAh g^{-1} and 800 mAh g^{-1}, respectively (Fig. 16). In contrast, the first charge capacity of Al NR on Ti substrate was 400 mAh g^{-1} (Fig. 17). After 10 cycles, the Al NR on new substrate retained 500 mAh g^{-1} of discharge capacity (Fig. 16), while the Al NRs on the Ti substrate only discharged 100 mAh g^{-1} (Fig. 17). The SEM of the cross section of Al NRs on new substrate shows no peel-off or detachment (Fig. 18) resulting in a better cycleability. It is obvious that the selection of

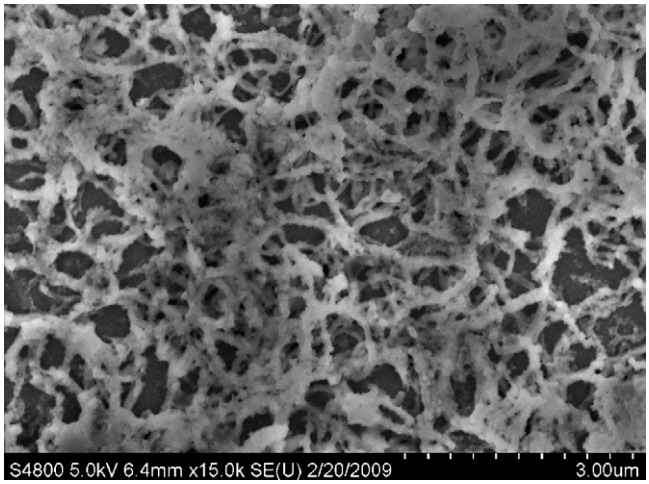

Fig. 12. SEM Image of the Al NRs after 100 cycles (15,000×).

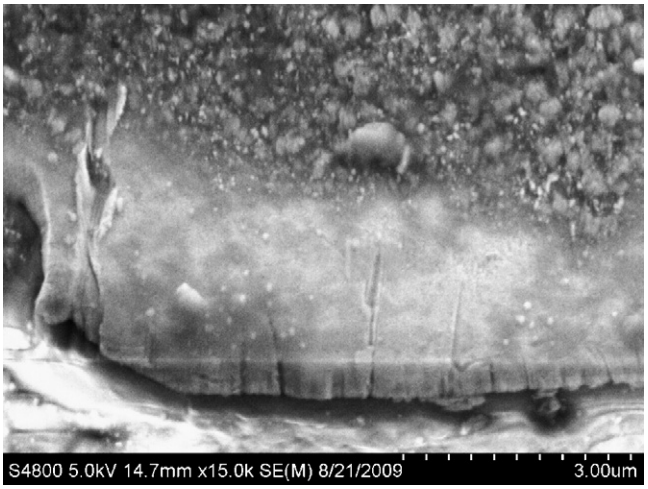

Fig. 13. The cross section of the Al NRs on Ti substrate after 100 cycles (15,000×).

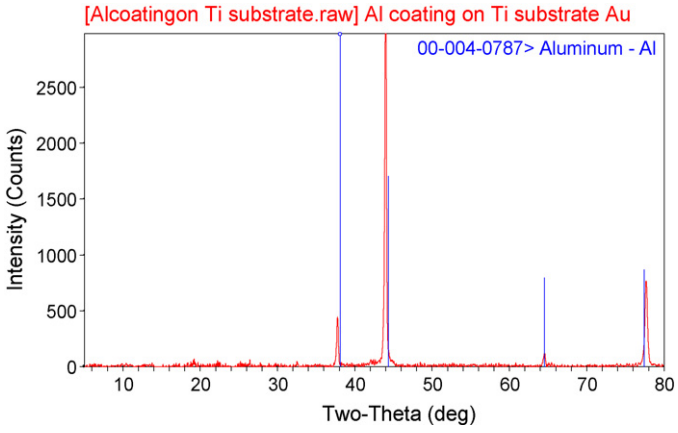

Fig. 14. XRD of the Al NRs on Ti substrate after 100 cycles.

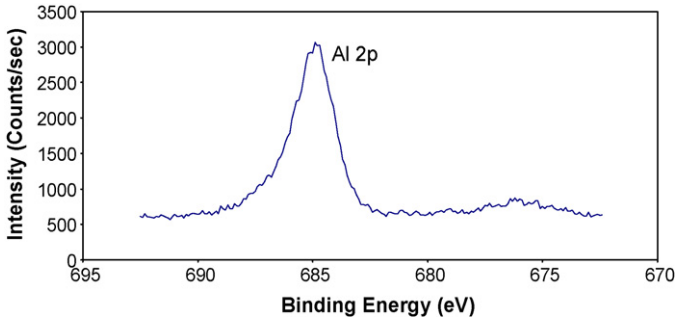

Fig. 15. XPS of Al NRs anode after 100 cycles.

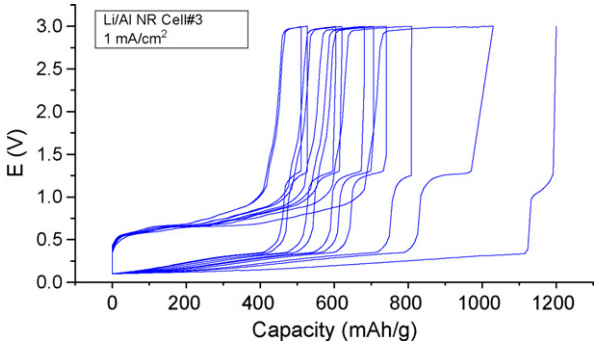

Fig. 16. Ten cycles of Al NRs on new substrate.

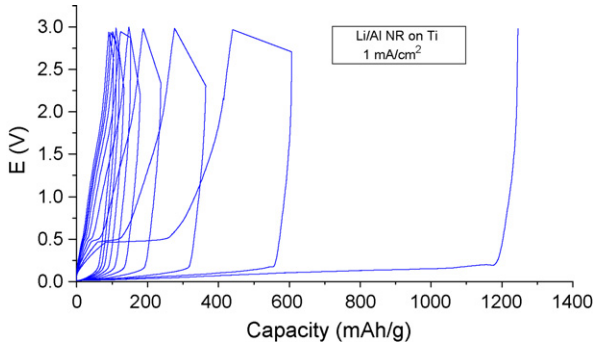

Fig. 17. Ten cycles of Al NRs on Ti substrate.

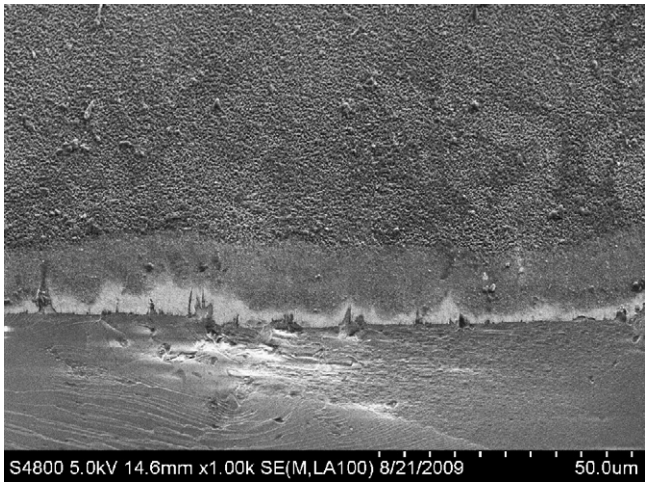

Fig. 18. The cross section of the Al NRs on Cu substrate after 100 cycles (10,000×).

the substrates influences the cycleability of Al NR anode considerably. It is indicated that optimal selection of substrate may lead to sustainable high capacity of the anodes made by Al or other metal nanorods. The details on how to select the right substrate will be discussed in future papers.

4. Conclusions

The anodes made by aligned Al NRs grown on electrodes directly demonstrated high discharge capacities of 1243 mAh g^{-1} at the rates of 0.5 C in the Li-ion rechargeable cells, which is close to the theoretical electrochemical capacity (1411 mAh g^{-1}) of a Li/Al battery. The high capacity initially observed decreased rapidly in charge–discharge cycling. It was found that the changes of crystalline structure and morphology might be partially responsible for the capacity decay. Further investigation revealed that changing the material of the substrates improved cycleability significantly. The optimal selection of substrate materials will lead to sustainable high capacity for thin file of nanostructured anodes.

Acknowledgements

This work is financially supported by Savannah River National Laboratory LDRD program. Savannah River National Laboratory is operated by Savannah River Nuclear Solution for US Department of Energy under contract DE-AC09-08SR22470.

References

[1] D. Linden, Handbook of Batteries, 2nd ed., McGraw-Hill, 1994.
[2] I. Sandu, et al., Solid State Ionics 178 (2007) 1297–1303.
[3] N. Dimov, et al., J. Power Sources 171 (2007) 886–893.
[4] E. Hosono, et al., J. Electroanal. Chem. 154 (2) (2007) A146–A149.
[5] K. Ui, et al., J. Power Sources 189 (2009) 224–229.
[6] X. Let, et al., J. Alloys Compd. 429 (2007) 311–315.
[7] C.C. Chang, et al., J. Phys. Chem. C 111 (2007) 16423–16427.
[8] N. Li, et al., J. Power Sources 97–98 (2001) 240–243.
[9] Y.-M. Kang, et al., J. Power Sources 133 (2004) 252–259.
[10] S.-H. Lee, et al., Adv. Mater. 18 (2006) 763–766.
[11] Y.-P. Zhao, et al., Proc. SPIE. in: A. Lakhtakia (Ed.), Nanotubes & Nanowires, Bellingham, WA, 2003.
[12] E.A. Brades, G.B. Brook (Eds.), Smithells Metals Reference Book, 7th edition, Butterworth-Heinemann, 1998.